Structures

Optimal Design of Cold-Formed Steel Lipped Channel Beams: Combined Bending, Shear, and Web Crippling

Perampalam Gatheeshgar
Faculty of Engineering and Environment, Northumbria University,
Newcastle upon Tyne, UK.

Keerthan Poologanathan
Faculty of Engineering and Environment, Northumbria University,
Newcastle upon Tyne, UK.

Shanmuganathan Gunalan
School of Engineering and Built Environment, Griffith University,
Gold Coast Campus, Australia.

Islam Shyha
Faculty of Engineering and Environment, Northumbria University
Newcastle upon Tyne, UK.

Konstantinos Daniel Tsavdaridis
School of Civil Engineering, Faculty of Engineering and Physical Sciences, University of Leeds,
Leeds, UK

Marco Corradi
Faculty of Engineering and Environment, Northumbria University
Newcastle upon Tyne, UK.

Abstract

The load carrying capacity of cold-formed steel (CFS) beams can be enhanced by employing optimisation techniques. Recent research studies have mainly focused on optimising the bending capacity of the CFS beams for a given amount of material. However, to the best of authors' knowledge, very limited research has been performed to optimise the CFS beams subject to shear and web crippling actions for a given amount of material. This paper presents the optimisation of CFS lipped channel beams for maximum bending, shear, and web crippling actions combined, leading to a novel conceptual development. The bending, shear and web crippling strengths of the sections were determined based on the provisions in Eurocode 3, while the optimisation process was performed by the means of Particle Swarm Optimisation (PSO) method. Combined theoretical and manufacturing constraints were imposed during the optimisation to ensure the practicality of optimised CFS beams. Non-linear Finite Element (FE) analysis with imperfections was employed to simulate the structural behaviour of optimised CFS lipped channel beams after successful validation against previous experimental results. The results demonstrated that, the optimised CFS sections are more effective (bending, shear,

and web crippling actions resulted in 30 %, 6 %, and 13 % of capacity increase, respectively) compared to the conventional CFS sections with same amount of material (weight). The proposed optimisation framework can be used to enhance the structural efficiency of CFS lipped channel beams under combined bending, shear, and web crippling actions.

Keywords: Cold-Formed Steel Beams; Bending Strength; Shear Strength; Web Crippling Strength; Combined Optimisation; Finite Element Analysis.

1 Introduction

Cold-formed steel (CFS) members offer more economical and efficient design solutions as they offer high strength-to-weight ratio, leading to material savings. Consequently, CFS members have been widely employed in a broad range of civil and structural engineering applications. The structural applications mainly include basic building elements for on-site assembly or prefabricated floor and wall panels, as well as volumetric modular units. However, due to their limited thickness, CFS members are highly prone to buckling instabilities. Prominent consideration is, therefore, given during the design process.

CFS beams are used as primary and secondary load-bearing elements. They fail majorly in bending, shear, web crippling or a combination of the above. Many research studies have performed experimental works [1-5] and numerical studies [6-12] to examine the ultimate cross-sectional resistance strength and behaviour of the CFS beams subject to the aforementioned prominent and combined actions. In particular, Fig. 1 depicts all possible failure modes of CFS beams. The sophisticated improvements in manufacturing technologies along with the cross-sectional flexibility nature of CFS lead to necessitated modifications into the CFS profiles.

In recent years, optimisation techniques have also been employed to enhance the bending performance of CFS beams. Such increased research focus resulted in novel CFS beam shapes with enhanced bending capacities. For example, Ye et al. [13, 14] optimised the lipped channel beams with intermediate web stiffeners and return lips, and introduced a novel folded-flange section. Gatheeshgar et al. [15-17] performed optimisation studies of CFS sections and introduced optimised super-sigma sections which can bear approximately 65% higher bending capacity compared to the conventional lipped channel beam with the same amount of material. They also investigated the relevant shear and web crippling capacities of the optimised sections and found that the optimised novel sections performed poorly compared to the lipped channel beam with the same amount of material. Fig. 2 shows the novel optimised sections considering section moment capacity [13-16].

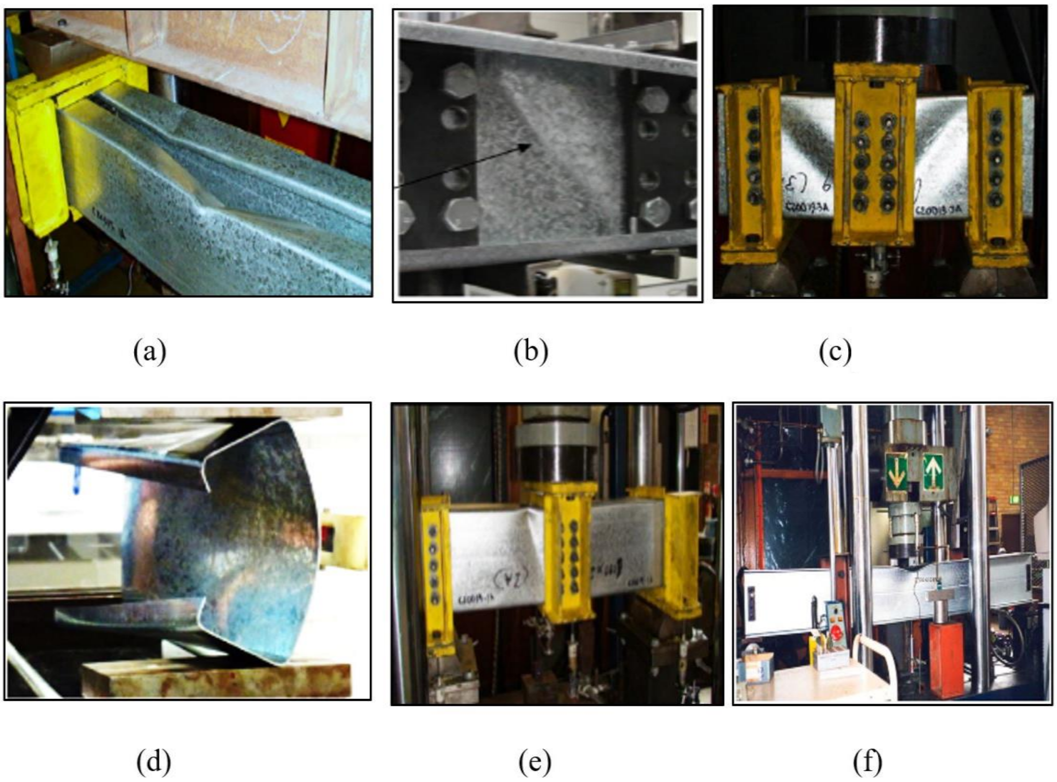

Fig.1 Different types of failure modes of CFS beams: (a) bending [1]; (b,c) shear [5, 6]; (d) web crippling [4]; (e) combined bending and shear [6]; (f) combined bending and web crippling [7].

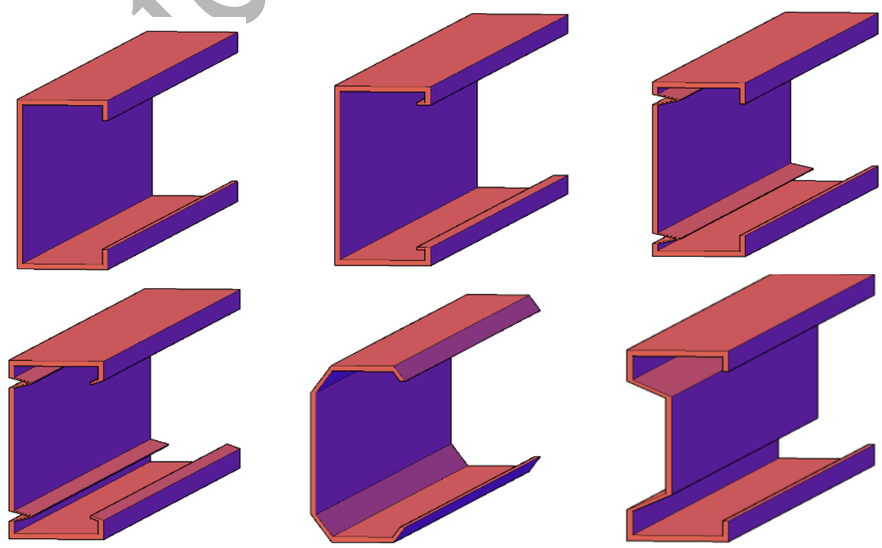

Fig. 2 Optimised CFS beam sections for bending maintaining the same amount of material [13-16].

It is worth to note that there are circumstances where CFS beams can fail not only predominantly in bending but also in shear, and web crippling actions. Shear failure is critical in short spans while web crippling failure occurs when CFS beams subjected to concentrated loads. Therefore, it is necessary to consider the shear and web crippling behaviour of the sections during the optimisation process. This will ensure the optimised beams can also perform efficiently under bending, shear, and web crippling, and thus they can be used in specific building applications.

The objectives of this paper are to (a) optimise the CFS lipped channel beams for bending, shear, and web crippling actions individually and (b) develop a novel concept of optimisation procedure to produce a lipped channel beam which can comparatively perform well in all three aforementioned actions. The optimisation was performed using Particle Swarm Optimisation (PSO) method and the objective functions were developed using Eurocode 3 [18, 19] guidelines. Finite Element (FE) models of lipped channel beams were developed and carefully validated against the test results. The validated FE models were then used to simulate the bending, shear, and web crippling strength and the combined behaviour of the optimised lipped channel beams. Finally, the optimised sections were compared with a commercially available lipped channel beam of the same amount of material (i.e., weight) to highlight any structural benefits. The potential advantages of employing specific optimisation techniques are also discussed via the analysed results and conclusions are drawn.

2 Eurocode 3 design rules for lipped channel beams

2.1 Bending

For the lipped channel beam, bending capacity was determined based on the effective width method provisions adopted in EN1993-1-3 [18] and EN1993-1-5 [19]. Both local and distortional buckling was taken into account in calculating the stiffness of the lipped channel beams. The local buckling effects of the internal compression (web and flange), and outstand compression (lip) elements were calculated based on the effective widths (compressive stress concentration at the corners) as defined in EN1993-1-5 [19]. The local and distortional buckling of a typical lipped channel beam is shown in Fig. 3. According to EN1993-1-5 [19] the effective width of the internal and outstand compression elements for local buckling can be calculated using a reduction factor on the plate width (ρ). Eqs. 1 and 2 provide the reduction factor values for internal and outstand compression elements, respectively.

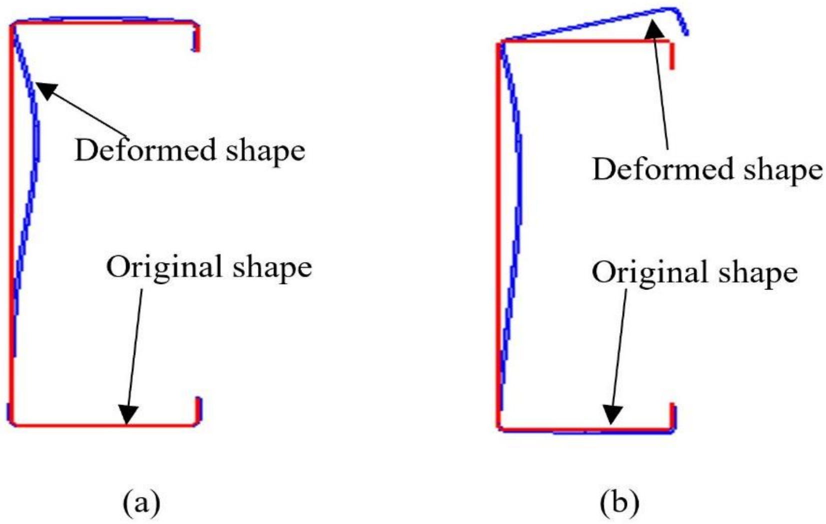

Fig. 3 Buckling types of a laterally braced CFS lipped channel beam subjected to bending stress: (a) local buckling; (b) distortional buckling.

$$\rho = \left[\frac{\lambda_p - 0.055(3+\psi)}{\lambda_p{}^2}\right] \quad (1)$$

$$\rho = \left[\frac{\lambda_p - 0.188}{\lambda_p{}^2}\right] \quad (2)$$

In Eqs. 1and 2, ψ is the ratio of the end stress in the plate element and λ_p is the slenderness ratio (= $\sqrt{f_y/\sigma_{cr}}$; f_y = yield strength and σ_{cr} is the elastic critical plate buckling stress).

In contrast to the cross-sectional width concept for local buckling, the distortional buckling of the flange-lip juncture is taken into consideration through reducing the effective plate thickness. The distortional buckling effect in lipped channel beam is mainly governed by the elastic critical stress of the edge stiffener ($\sigma_{cr,s}$). This is calculated simulating the restrain provided by the adjacent plates into a spring stiffness (K) and determining the effective cross-section area (A_s) and second moment of area (I_s) of the edge stiffener. The corresponding Young's modulus of the material (E) also needs to be used (see Eq.3). The reduction factor for the distortional buckling (χ_d) is obtained from the slenderness ratio, and $\sigma_{cr,s}$ is to be used for this. The strength of the effective area of the stiffener is then reduced by χ_d. This aforementioned step needs to be repeated until the convergence of χ_d.

$$\sigma_{cr,s} = \frac{2\sqrt{KEI_s}}{A_s} \quad (3)$$

For the laterally braced beams, the ultimate bending capacity ($M_{c,Rd}$) is the minimum of the bending capacity subject to local and distortional buckling failure.

2.2 Shear

The shear resistance capacity of the CFS lipped channel beams majorly depends on the web buckling and the contribution from the flange is likely to be negligible [5]. According to EN1993-1-5 [19] the design shear resistance ($V_{b,Rd}$) is given by the sum of web shear resistance ($V_{bw,Rd}$) and flange shear resistance ($V_{bf,Rd}$), as given in Eq. 4. Eq. 5 provides the formula for web shear resistance.

$$V_{b,Rd} = V_{bw,Rd} + V_{bf,Rd} \leq \frac{\eta f_{yw} h_w t}{\sqrt{3}\,\gamma_{M1}} \tag{4}$$

$$V_{bw,Rd} = \frac{\chi_w f_{yw} h_w t}{\sqrt{3}\,\gamma_{M1}} \tag{5}$$

where f_{yw} is the yield stress of the web, h_w is the clear web depth between the flanges and t is the thickness of the plate. EN1993-1-5 [19] recommends the value of 1.20 for η up to the steel grade S460 and value of 1.0 for higher steel grades. γ_{M1} is the partial factor. χ_w is the shear buckling reduction factor for the web. The web was assumed to be a rigid end post condition when calculating the shear buckling reduction factor of the web, χ_w. Moreover, the condition of transverse web stiffeners at supports and intermediate span was considered to determine the slenderness ratio (λ_w). The equation for the slenderness ratio is as follows:

$$\lambda_w = \frac{h_w}{37.4 t \varepsilon \sqrt{k_\tau}} \tag{6}$$

Where ε and k_τ denote the factor depending on f_{yw} and minimum shear buckling coefficient of the web panel, respectively. Annex A of EN1993-1-5 [19] carries the equations (see Eqs. 7 and 8) for the shear buckling coefficient (k_τ) of plates with rigid transverse stiffeners and without longitudinal stiffeners in terms of the distance between transverse stiffeners (a) and clear web depth between the flanges (h_w).

$$k_\tau = 5.34 + \frac{4.00}{(a/h_w)^2} \quad for\ \frac{a}{h_w} \geq 1 \tag{7}$$

$$k_\tau = 4.00 + \frac{5.34}{(a/h_w)^2} \quad for\ \frac{a}{h_w} < 1 \tag{8}$$

Even though provisions for the contribution from the flange on shear capacity are given in EN1993-1-5 [19], they were not considered in this study as the flange contributes a relatively small proportion to the total shear resistance [5, 20]. Their investigations showed that for most of the lipped channel sections the condition to consider the contribution to the shear capacity from flange cannot be met and for the sections which meet the condition, the calculated shear contribution from flange is negligible.

2.3 Web crippling

Web crippling failure occurs when CFS beams are subjected to concentrated loads. EN1993-1-3 [18] categorises the web crippling failure of the cross-sections with single web into four groups depending on the load cases: End-Two-Flange (ETF), Interior-Two-Flange (ITF), End-One-Flange (EOF), and Interior-One-Flange (IOF). However, only the ETF load case was considered in this study. Because for a typical section with a lower thickness, web crippling strength is lower for ETF load case compared to other load cases based on EN1993-1-3 [18] calculations. Eq. 9 presents the web crippling strength ($R_{w,Rd}$) as given in EN1993-1-3 [18]. This equation is valid for the cross-sections that comply with $r/t \leq 6$ (r=internal radius) and $h_w/t \leq 200$ conditions.

$$R_{w,Rd} = \frac{k_1 k_2 k_3 \left[6.66 - \frac{h_w/t}{64}\right]\left[1 + 0.01\frac{S_s}{t}\right] t^2 f_y}{\gamma_{M1}} \quad (9)$$

Where the values of the coefficient are determined such that k_1=1.33-0.33k where k=f_y/228, k_2=1.15-0.15(r/t) but 0.5≤k_2≤1.0, and k_3=1 for lipped channel beams. S_s is the nominal length of the bearing plate. A graphical illustration for the cross-sectional dimensions is depicted in Fig.4. It is worth to note that EN1993-1-3 [18] carries no separate equations for fastened and unfastened situations for ETF load case. Therefore, as a conservative approach, the flanges unfastened condition was considered in this study.

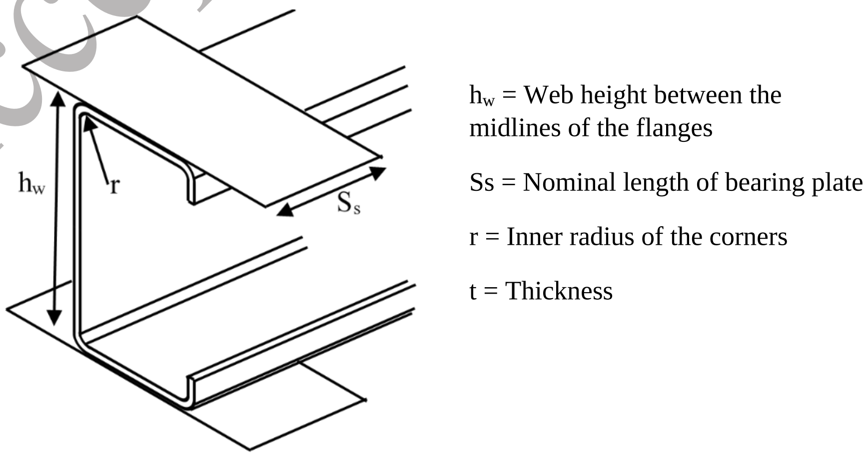

Fig. 4 Graphical illustration of the cross-sectional dimensions for ETF load case web crippling

3 Optimisation procedure for bending, shear, and web crippling

3.1 General

This section provides details on the formulation of the optimisation problem under different conditions and implemented practical and manufacturing constraints. Optimisation is nowadays an important approach to obtain economical designs with enhanced structural efficiency. The PSO algorithm was used to perform the optimisation while the cross-section resistant capacity design equations discussed in section 2 were used as objective functions. Extensive detail on the description of PSO optimisation can be found in the literature [13-16]. A commercially available lipped channel beam was set as a reference section (see Fig. 5). This section has a total coil length of 415 mm and thickness of 1.5 mm. The yield strength, Young's modulus, and Poisson's ratio of the reference section are 450 MPa, 210 GPa, and 0.3, respectively. Similar cross-sectional (coil length and thickness) and mechanical properties (yield strength, Young's modulus, and Poisson's ratio) were adopted in the optimisation process to assess the degree of improvement of the optimised sections for a given amount of material used.

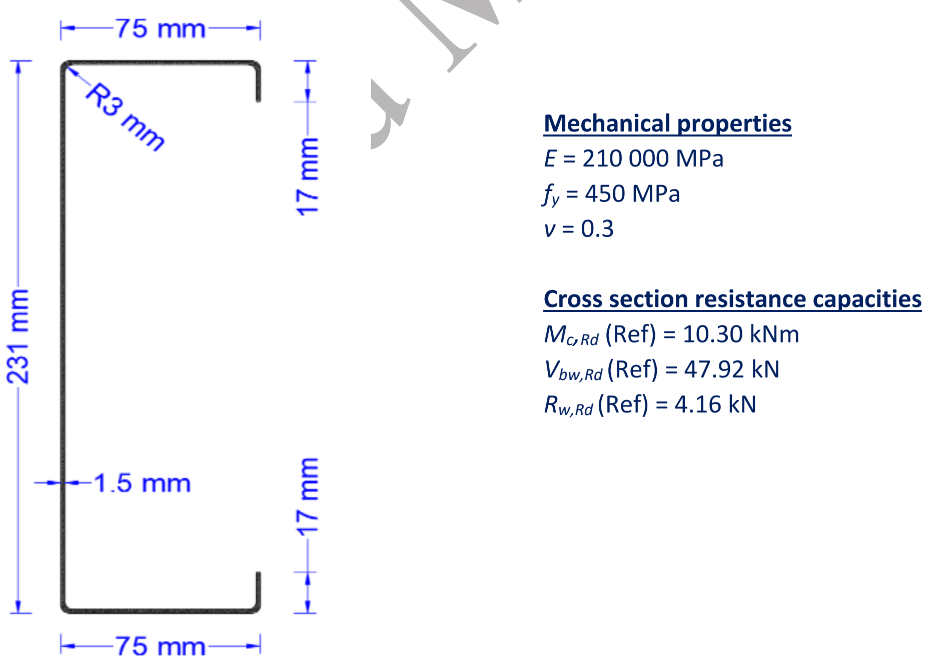

Fig. 5 Dimensions, mechanical properties, and cross-section resistance capacities of the reference section.

3.2 Optimisation formulation for bending

As discussed in section 2.1, the bending failure of a CFS beam can occur subject to local and distortional buckling failures, assuming that beam is laterally braced. The objective function is formulated such that considering the minimum of local and distortional buckling capacities. The flange (*b*), web (*h*) and lip (*c*) length were considered as design variables during the optimisation for bending. The objective function for bending is defined by:

$$Maximize\ [M_{c,Rd}(x)] = W_{eff}(x).\, f_y/\gamma_{M1} \tag{10}$$

Where $M_{c,Rd}\,(x)$ is the section moment capacity of the lipped channel beam for each design variable. $W_{eff}\,(x)$ is the section modulus of the lipped channel section. These variables were set to vary within the theoretical and manufacturing constraints.

3.3 Optimisation formulation for shear

To formulate the objective function to determine the shear capacity of the lipped channel beams, Eq. 5 was used. During the optimisation, only the web height was considered as design variable as the contribution from the flange is negligible, as explained in section 2.2. The objective function to optimise the shear capacity is defined by:

$$Maximize\ [V_{bw,Rd}(x)] = \frac{\chi_w(x) f_{yw} h_w(x) t}{\sqrt{3}\,\gamma_{M1}} \tag{11}$$

Where all the variables are defined similar in section 2.2.

3.4 Optimisation formulation for web crippling

Similar to shear behaviour, according to the provisions provided in Eurocode 3 [18, 19], the web crippling strength of the lipped channel beam is also mainly governed by the web. Therefore, only the dimension of the web was considered as variable during the optimisation. The considered objective function for the optimisation is given in Eq. 12.

$$Maximize\ [R_{w,Rd}(x)] = \frac{k_1 k_2 k_3 \left[6.66 - \frac{h_w(x)/t}{64}\right]\left[1 + 0.01\frac{S_s}{t}\right] t^2 f_y}{\gamma_{M1}} \tag{12}$$

Where all the variables are defined as similar in section 2.3 and Fig 4. A value of 100 mm was selected for the length of the bearing plate, S_s. This length was selected to avoid the flange crushing behaviour which has substantial influence in the web crippling capacity for low value of S_s [8].

3.5 Optimisation formulation for overall/combined performance

The concept of combined optimisation of lipped channel beam is necessary to enhance the overall performance of the cross-section. Lee et al. [21] developed an optimum design procedure using micro genetic algorithm for simply supported CFS beams subjected to uniformly distributed loads. They aimed to reduce the weight of the CFS beam section subject to defined magnitude of distributed load to satisfy the bending, shear, web crippling, and deflection criteria. However, the optimisation was performed for un-lipped channels. Therefore, this study intends to develop a combined optimisation methodology under ultimate limit state conditions for lipped channel beams. The general design procedure for a lipped channel beam includes bending, shear, and web crippling failure considerations. The aim is to develop an optimised section with a maximised capacity which can over-perform under all bending, shear, and web crippling actions compared to the reference section (depicted in Fig. 5) while having the same amount of material. Therefore, all the objective functions developed in section 3.1, 3.2, and 3.2 were combined to produce a unified objective function. The web, flange, and lip dimensions were considered as the design variables. Eq. 13 represents the developed unified objective function for combined optimisation.

$$Max\ [MVR(x)] = \left(\frac{M_{c,Rd}\ (x)}{M_{c,Rd(Ref)}}\right) + \left(\frac{V_{bw,Rd}(x)}{V_{b,Rd\ (Ref)}}\right) + \left(\frac{R_{w,Rd}(x)}{R_{w,Rd(Ref)}}\right) \tag{13}$$

$$Subjected\ to: \quad \left(\frac{M_{c,Rd}\ (x)}{M_{c,Rd(Ref)}}\right) \geq 1.0$$

$$\left(\frac{V_{bw,Rd}(x)}{V_{b,Rd\ (Ref)}}\right) \geq 1.0$$

$$\left(\frac{R_{w,Rd}(x)}{R_{w,Rd(Ref)}}\right) \geq 1.0$$

Eq. 13 has been developed adding three ratios pertaining to bending, shear, and web crippling. These are the ratios between the relevant capacity of optimised sections and relevant capacity of the reference section (Fig. 4) for bending, shear, and web crippling, accordingly. Each ratio was set to be greater than 1.0 in order to obtain the optimum lipped channel section with higher capacities compared to the reference lipped channel section. This combined optimisation resulted in promising results, as none of the capacities was reduced compared to their corresponding reference lipped channel beam capacities. Table 1 and Fig. 6 present the optimised capacities of the lipped channel beams with the same amount of material for bending, shear, web crippling and combined actions and the corresponding optimised dimensions, respectively. The performance of optimised lipped channel beams is illustrated in Fig. 7.

Table 1: Results of the optimised bending capacities for bending, shear, and combined performance (Capacities based on Eurocode3)

Actions interested in optimisation	Optimised capacities and other capacities			Reference and optimised dimensions			Performance factor			
	$M_{c,Rd}$ (kNm)	$V_{b,Rd}$ (kN)	$R_{w,Rd}$ (kN)	Web (mm)	Flange (mm)	Lip (mm)	$M_{c,Rd}$ / $M_{c,Rd(Ref)}$	$V_{b,Rd}$ / $V_{b,Rd(Ref)}$	$R_{w,Rd}$ / $R_{w,Rd(Ref)}$	Total (Eq.13)
Reference (Fig. 5)	10.30	47.92	4.16	231	75	17	1.00	1.00	1.00	3.00
Bending (Eq. 10)	13.38	49.96	3.75	270	50	22.5	1.30	1.04	0.90	3.24
Shear (Eq. 11)	12.51	50.63	3.59	286	50	15	1.21	1.06	0.86	3.13
Web crippling (Eq. 12)	8.62	44.33	4.68	179	90	28	0.84	0.93	1.13	2.90
Combined (Eq. 13)	11.59	47.92	4.16	231	64	28	1.12	1.00	1.00	3.12

Note: $M_{c,Rd}$ = Section moment capacity, $V_{b,Rd}$ = Shear resistance, $R_{w,Rd}$ = Web crippling strength, $M_{c,Rd(Ref)}$= Section moment capacity of reference section, $V_{b,Rd(Ref)}$ = Shear resistance of reference section, $R_{w,Rd(Ref)}$= Web crippling strength of reference section.

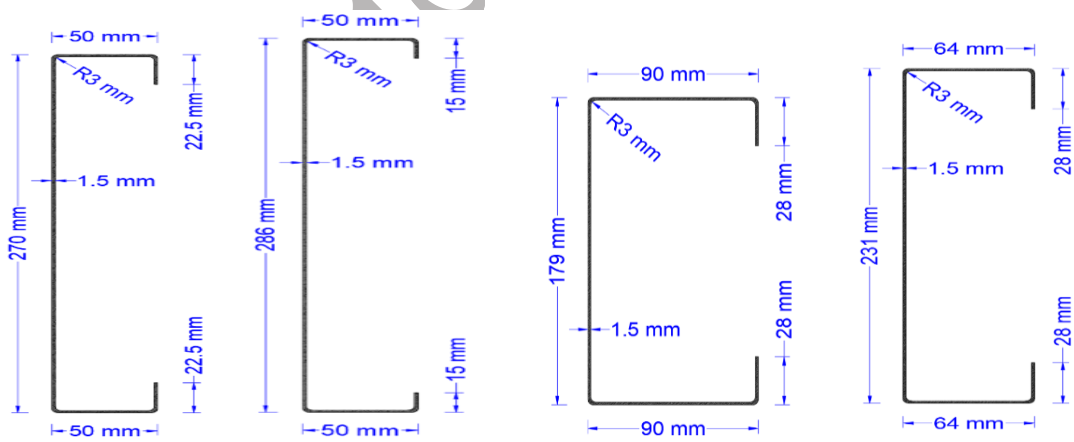

(a) (b) (c) (d)

Fig. 6 Dimensions of the optimised lipped channel beams under given constrains for considering individual and overall behaviour: (a) bending; (b) shear; (c) web crippling; (d) combined.

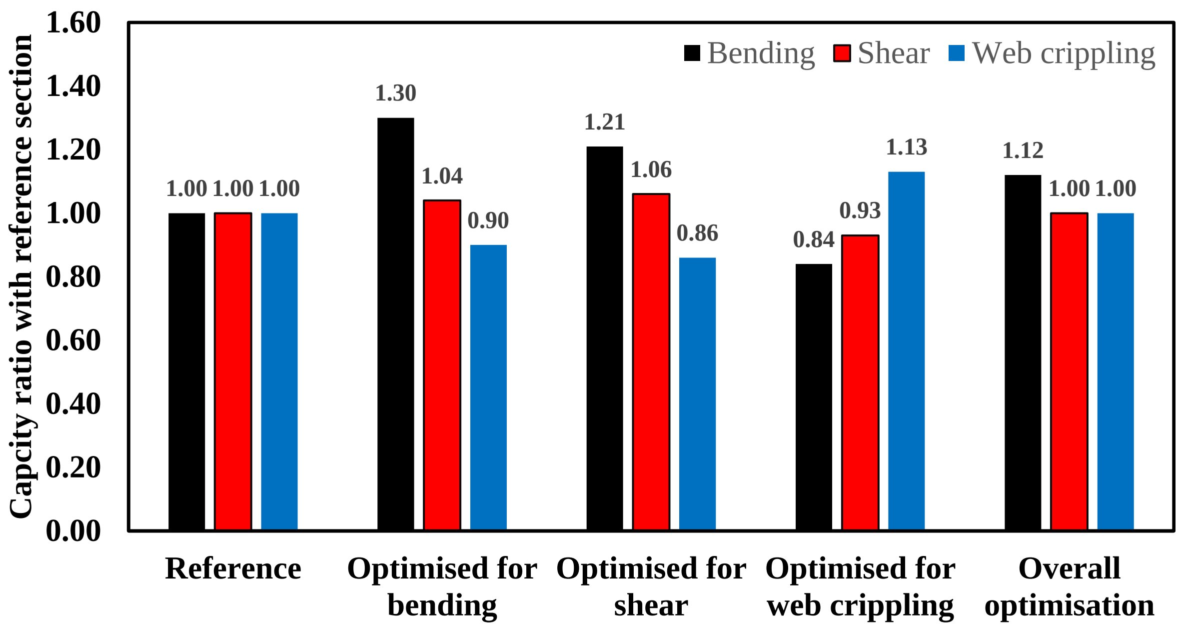

Fig. 7 Performance of optimised lipped channel beams

3.6 Imposed theoretical and manufacturing constraints

Theoretical and manufacturing constraints guide the optimisation to ensure the practicality of the resultant (optimum) dimensions of the lipped channel beams. The constraints for the optimisation were set in line with Eurocode 3 [18, 19] and current construction practices. EN1993-1-3 [18] states the following dimensional constraints for CFS beams: $b/t \leq 60$, $c/t \leq 50$, $0.2 \leq c/t \leq 0.6$, and $h/t \leq 500$ in usual notations. These constraints were fed into the optimisation problem. Regarding the practical and manufacturing constraints and in order to find out the bounds of the segments of lipped channel beams, a survey was conducted with help from an industrial partner to assess the dimensional limitations of the commercially available lipped channel beams. In total 530 lipped channel profiles from 17 different manufacturers across the UK were analysed and the range of the dimensional and mechanical values was mapped. Table 2 presents the findings of the survey on commercially available lipped channel beams. Combining the dimensional bounds obtained from the survey alongside with manufacturing constraints reported by Ye et al. [13], additional constraints were imposed. Even though the flange dimensions vary in between 34 mm and 125 mm, the lower bound was set to 50 mm to ensure the proper connection of the joist with floorboards and trapezoidal decking [13]. While the upper bound was set in line with Eurocode 3 [18, 19] limit. For the lip, the lower and upper bounds were selected as 15mm [13] and 28 mm, respectively. The length of the web was decided based on the coil length, web, and flange length. However, the height of the web was limited to 300 mm and the minimum height of the web was set to 100 mm in order to ensure connection plates can be fixed.

Table 2: Dimensional and yield strength bounds of commercially available lipped channel beams.

Profile parameters	Range
Web (mm)	60 – 500
Flange (mm)	34 – 125
Lip (mm)	7 – 28
Radius (mm)	0.9 – 8
Thickness (mm)	0.6 – 5
Coil length (mm)	154 – 750
Yield strength (MPa)	320 – 550

4 FE analysis and results

4.1 FE model

The bending, shear, and web crippling capacities of the reference and optimised lipped channel beams were also obtained using a commercially available FE software, ABAQUS version 2017 [22]. FE analysis was aimed to verify the proposed optimisation approach and to investigate the pre-buckling and post-buckling behaviours of the optimised lipped channel beams. For bending and shear, the whole analysis procedure included two phases: eigenvalue buckling analysis and non-linear analysis. For bending and shear models, initial geometric imperfections were applied to the critical buckling mode (the lowest) obtained from the linear buckling analysis while the imperfection magnitude was chosen according to Schafer and Pekoz [23]. For web crippling models, it was found that the effect of imperfection on web crippling strength was negligible. Therefore, imperfections were not incorporated into the FE models. Sundararajah et al.'s [8] finding also demonstrated that the effect of imperfection on web crippling capacity is negligible (<1%) for two flange load cases.

A four-point bending arrangement was used for the bending tests. This set-up ensures the pure bending failure of the lipped channel beam at the mid-span with the absence of the shear force. Three-point bending set-up was used to simulate the lipped channel beam subject to shear. Herein, prominent shear failure was ensured by selecting the aspect ratio (=shear span/clear web depth) equal to unity. However, to develop the web crippling FE model under ETF load case, extrusion length of $3d_1$ [4], where d_1 denotes the length of the flat portion of the web, was used. Fig. 8 shows the schematic diagram of the FE models constructed in ABAQUS for bending, shear, and web crippling, while Table 3 presents the adopted boundary conditions. The load was applied in terms of displacement control at the loading points, while simply supported boundary conditions were adopted. In bending models, lateral restraints were provided at regular intervals (at top and bottom flanges) to restrain the lateral-torsional buckling of the lipped channel beams, while in shear models, straps were simulated as boundary conditions in flanges adjacent to the web side plates. The web side plates, in bending and shear models, were connected using the 'tie' constraint option available in ABAQUS. On the other hand, in web crippling models, bearing plates were connected using the 'hard' contact alongside with the input of friction coefficient 0.4.

Material modelling is a key parameter. Haidarali and Nethecot [10] investigated four different material models to identify the suitable stress-strain relationship for FE modelling. They concluded that CFS material exhibits negligible strain hardening while the gradual yielding of the material is essential in FE modelling. Siahaan et al. [24], Keerthan and Mahendran [25], and Sundararajah et al. [8] successfully employed a bi-linear stress-strain curve with nominal yield point and no strain hardening in the FE modelling of CFS beams subject to bending, shear, and web crippling. Therefore, the stress-strain behaviour of the CFS beam was assumed to be with an elastic-perfect plastic model with nominal yield-stress considering the negligible stain-hardening in CFS. It is worth to mention that the effect of the residual stresses and corner strength enhancement were not inputted into the FE models as both can approximately counter affect each other [26].

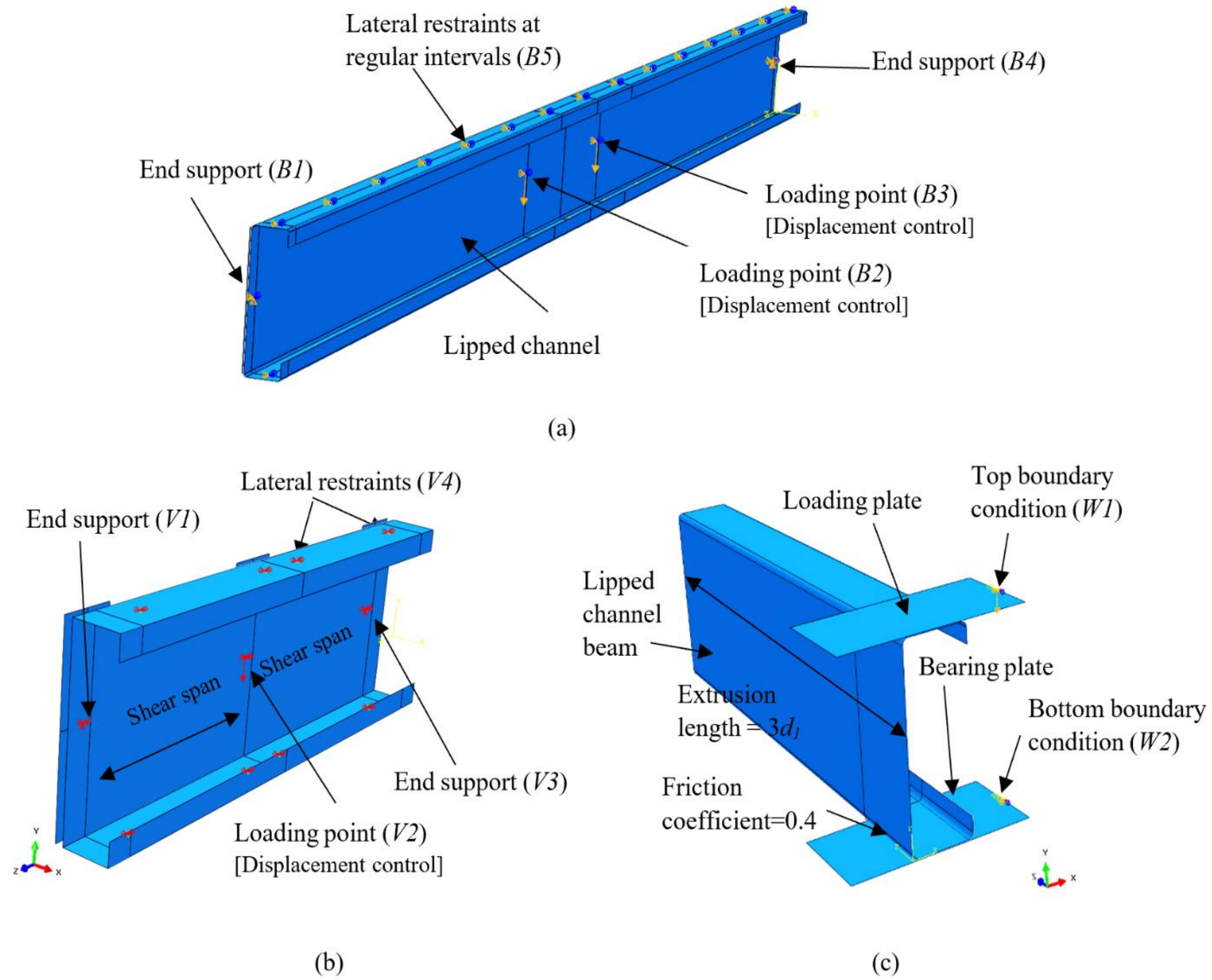

Fig. 8 Schematic diagram of the developed FE models with boundary conditions: (a) bending; (b) shear; (c) web crippling.

A quadrilateral shell element with reduced integration, aka S4R in ABAQUS element library, was employed for all analyses. Fig. 9 depicts the element types and mesh sizes of the FE models. The lipped channel beams were refined with 5 mm × 5 mm mesh size. Finer mesh size (1 mm × 5 mm) was used in corner regions. The web side plates (in bending and shear models) and bearing plates (in web crippling model), which are used to provide the boundary conditions and apply the load, were meshed with 10 mm × 10 mm element size. In addition, bearing plates were modelled using R3D4 rigid plate elements. These type of element types and mesh sizes were successfully used in past research studies on FE modelling of CFS beams [6, 8, 9, 13, 15, 16, 27, 28]. The selected mesh sizes showed a good agreement with test results during the validation process.

Table 3: Adopted boundary conditions in FE models

Locations marked in Fig.8	Boundary conditions					
	Translations			Rotations		
	UT_x	UT_y	UT_z	UR_x	UR_y	UR_z
Bending						
B1	Restrained	Restrained	Restrained	Free	Free	Restrained
B2	Restrained	Free	Free	Free	Free	Restrained
B3	Restrained	Free	Free	Free	Free	Restrained
B4	Restrained	Restrained	Free	Free	Free	Restrained
B5	Restrained	Free	Free	Free	Free	Restrained
Shear						
V1	Restrained	Restrained	Restrained	Free	Free	Restrained
V2	Restrained	Free	Free	Free	Free	Restrained
V3	Restrained	Restrained	Free	Free	Free	Restrained
V4	Restrained	Free	Free	Free	Free	Restrained
Web crippling						
W1	Restrained	Free	Restrained	Free	Free	Restrained
W2	Restrained	Restrained	Restrained	Free	Free	Restrained

Note: UT_x = Translation in x-direction, UT_y = Translation in y-direction, UT_z = Translation in z-direction, UR_x = Rotation about x-axis, UR_y = Rotation about y-axis, UR_z = Rotation about z-axis

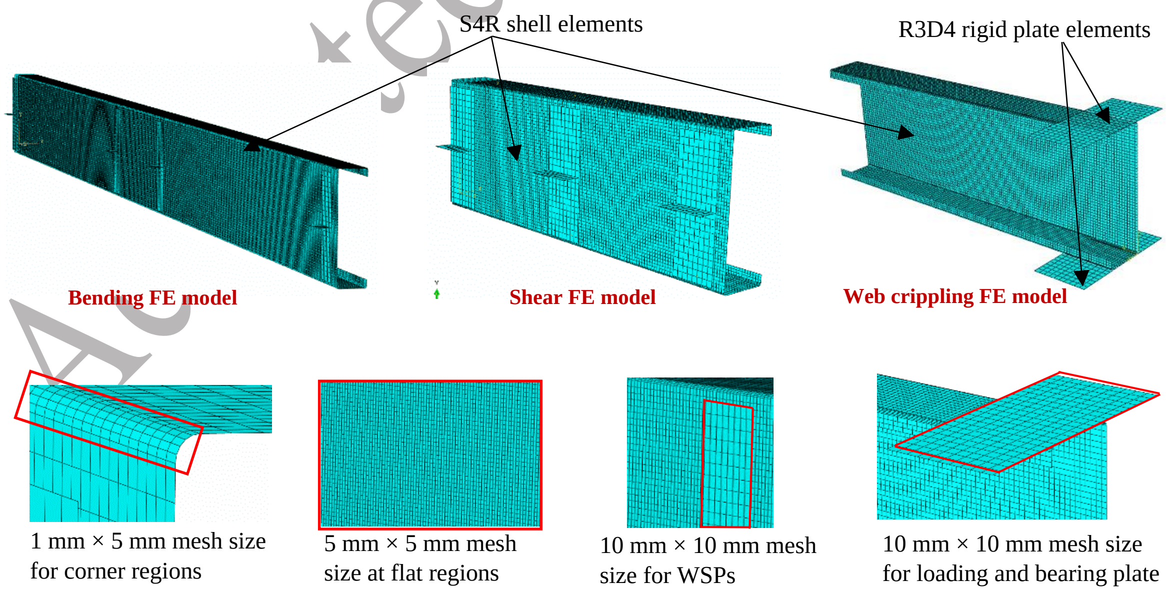

Fig. 9 Meshing outline and element types in FE models.

4.2 Validation of FE models

The aforementioned modelling characteristics were validated against the experimental results to ensure their capabilities in predicting accurately the cross-section resistance and behaviour. Pham and Hancock [1], Keerthan and Mahendran [5], and Sundararajah et al. [4] investigated the structural behaviour of the lipped channel beams subject to bending, shear and, web crippling through experimental studies. Six test results from each study were selected and validated against the FE results. Table 4 presents the comparison of ultimate moment capacities obtained from the FE analyses and test results. Section moment capacities obtained from FE analyses showed a good agreement with experiment bending test results with a mean value of 0.97 and a Coefficient of Variation (COV) value of 0.07. Further, the comparison between the shear resisting capacities obtained from FE analyses and Keerthan and Mahendran's [5] test results is presented in Table 5. The shear resisting capacity ratios of FE models and test results registered in a good agreement with a mean and a COV values of 0.99 and 0.08, respectively. The six web crippling test results for the ETF load case with 100 mm bearing plate was selected for the web crippling validation as in the optimisation procedure; similar bearing plate length was also selected. Table 6 compares the web crippling capacity generated from FE models and tests results. From the scatter of results (COV=0.05) and a mean value of 0.93, it can be concluded that FE models are capable of predicting web crippling strength.

Table 4: Comparison of experimental and FE section moment capacities

LCB specimen	h (mm)	b (mm)	c (mm)	r (mm)	t (mm)	f_y (MPa)	Test [1] (kNm)	FE (kNm)	Test/FE
Mw_C15015	152.70	64.77	16.57	5.00	1.50	514.10	9.5	9.6	0.99
Mw_C15019	153.38	64.47	16.00	5.00	1.90	534.50	12.9	13.6	0.95
Mw_C15024	152.60	62.70	19.70	5.00	2.40	485.30	17.7	16.6	1.08
Mw_C20015	203.70	76.08	16.42	5.00	1.50	513.40	12.2	13.3	0.92
Mw_C20019	202.60	77.92	17.28	5.00	1.90	510.50	18.9	21.3	0.89
Mw_C20024	202.35	76.61	20.38	5.00	2.40	483.50	27.8	27.6	1.01
Mean									0.97
COV									0.07

Note: h = Web depth, b = Flange width, c = Lip length, r = Corner inner radius, t = Thickness, fy = Yield strength

Table 5: Comparison of experimental and FE shear resistance capacities

LCB specimen	a/d_1	d_1 (mm)	t (mm)	f_y (MPa)	Test [5] (kN)	FE (kN)	Test/FE
160×65×15×1.90	1.0	156.8	1.92	515	73.8	77.58	0.95
200×75×15×1.50	1.0	197.0	1.51	537	57.0	61.90	0.92
160×65×15×1.50	1.0	157.5	1.51	537	54.5	55.20	0.99
120×50×18×1.50	1.0	116.8	1.49	537	43.3	47.80	0.91
200×75×15×1.95	1.0	198.0	1.93	271	55.1	50.07	1.10
120×50×18×1.95	1.0	118.6	1.95	271	38.1	34.88	1.10
Mean							0.99
COV							0.08

Note: a = Shear span, d_1 = Clear web depth, t = Thickness, f_y = Yield strength

Table 6: Comparison of experimental and FE web crippling strength under ETF load case

LCB specimen	l_b (mm)	f_y (mm)	t (mm)	r (mm)	t (mm)	b (mm)	c (mm)	h (MPa)	L (mm)	Test [4] (kN)	FE (kN)	Test/ FE
C10010	100	581	1.03	3.50	1.50	50.2	14	99.8	306	2.13	2.43	0.88
C10015	100	540	1.52	4.00	1.90	50.9	15.3	100.4	306	5.27	5.58	0.94
C15012	100	556	1.21	4.00	2.40	61.9	19.6	150.9	456	2.46	2.56	0.96
C15015	100	531	1.52	4.50	1.50	60	19.8	150	456	4.03	4.18	0.96
C20019	100	506	1.91	5.00	1.90	76.5	22	203.4	606	6.01	6.12	0.98
C20024	100	526	2.41	5.00	2.40	76.4	20.4	203.5	609	9.45	10.72	0.88
Mean												0.93
COV												0.05

Note: l_b = Bearing plate length, f_y = Yield strength, t = Thickness, r = Corner inner radius, b = Flange width, c = Lip length, h = Web depth, L = Specimen length.

Figs. 10-12 show the moment/force-displacement responses and failure mode comparisons for bending, shear, and web crippling, respectively. In Fig. 11, initial displacements obtained from FE analysis are associated with lower displacements in comparison to laboratory test curve. This is because the initial bolt slip which commonly occurs in laboratory tests. This is difficult to simulate in FE modelling. Similar variation in force-displacement behaviour between test and FE analysis has also been obtained by Pham and Hancock [6]. The trend of force-displacement responses and failure modes obtained from the FE models correlate reasonably well with the experimental results. Thus, pre-collapse, collapse, and post-collapse mechanisms can be well-approximated through developed FE models. This ensures the accuracy of the FE models predicting the cross-section resistance capacities. Therefore, the adopted FE model characteristics produced a satisfactory agreement with experiment results, in terms of ultimate cross-sectional resistance capacity prediction, force-displacement response, and failure mode comparison.

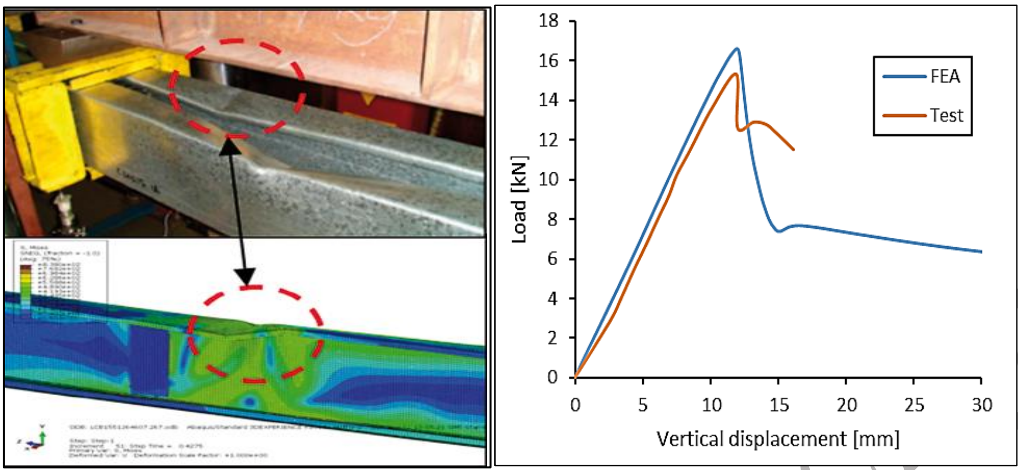

Fig. 10 Comparison of experimental [1] and FE bending failure modes and force-displacement behaviour for Mw_C20015 specimen

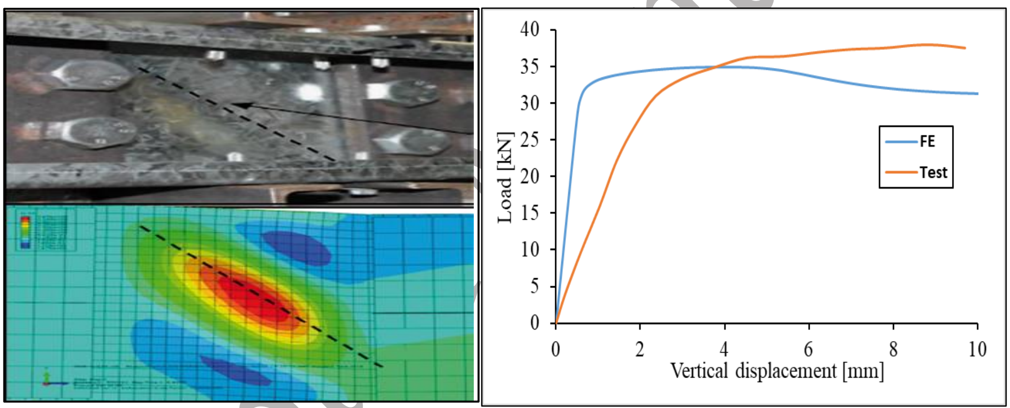

Fig. 11 Comparison of experimental [5] and FE shear failure modes and force-displacement behaviour for 120×50×18×1.95 specimen

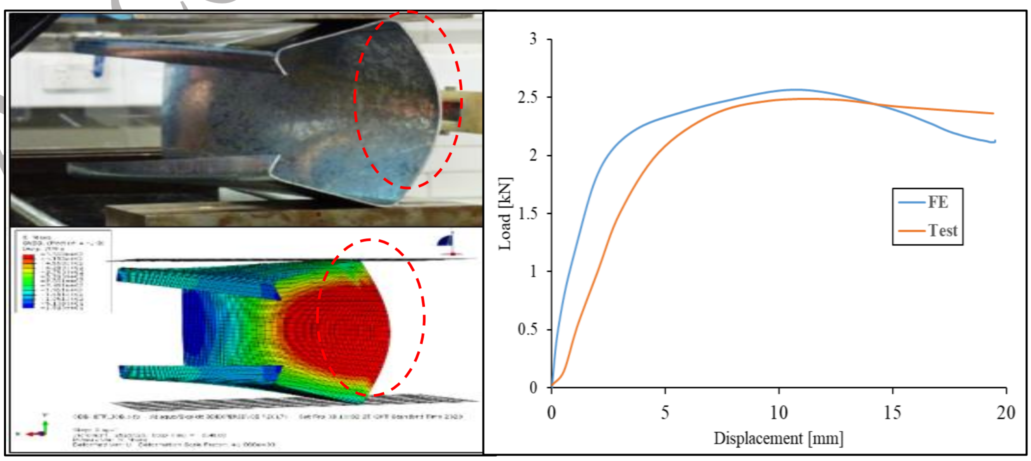

Fig. 12 Comparison of experimental [4] and FE web crippling failure modes and force-displacement behaviour for C15012 specimen

4.3 FE results

The validated FE models were then used to predict the strength and behaviour of the optimised lipped channel beams. Fig. 13 shows the stage-by-stage failure mode obtained from FE analysis for the optimised lipped channel beams for bending and its corresponding moment – displacement behaviour. Similarly, stage-by-stage failure modes obtained for the optimised lipped channel beams for shear and web crippling are illustrated in Fig. 14 and Fig. 15, respectively. The failure modes have shown a good illustration of the failure mechanism; failure at the compression flange for bending, diagonal failure for shear, and web buckling for web crippling. Moreover, the proposed optimisation approach can be verified by this FE analysis using the optimised sections. For that, the cross-sectional resistance capacities obtained from FE analyses were compared against the results obtained from Eurocode 3 (presented in Table 1). Table 7 presents the cross-sectional resistance capacities obtained from FE analyses for the optimised dimensions of lipped channel beams. The computational cross-section resistance capacities show a reasonable agreement with Eurocode 3 [18, 19] results except for the case for web crippling. Fig. 16 depicts the performance of the optimised lipped channel beams based on the FE results.

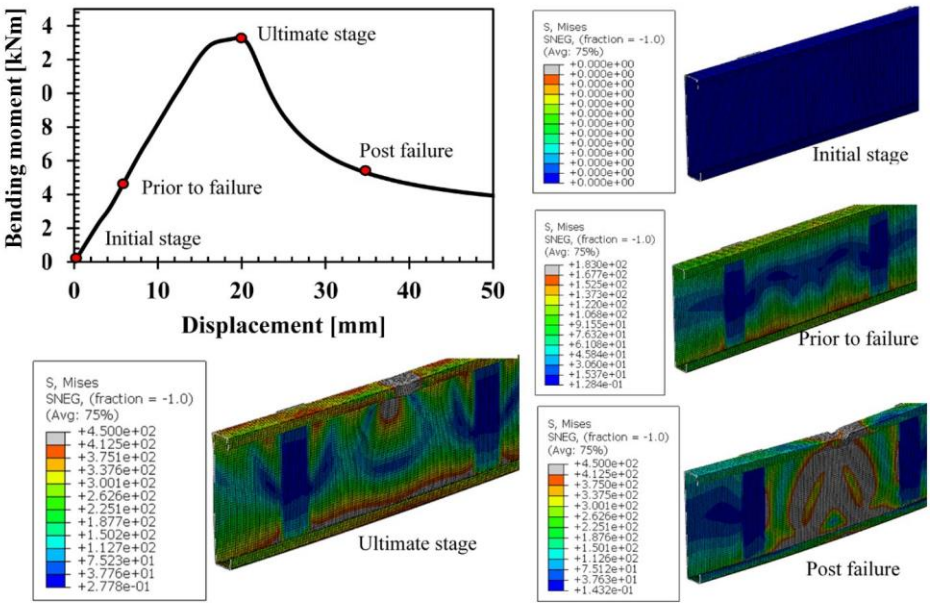

Fig. 13 Bending failure mode progression of optimised lipped channel beam for bending

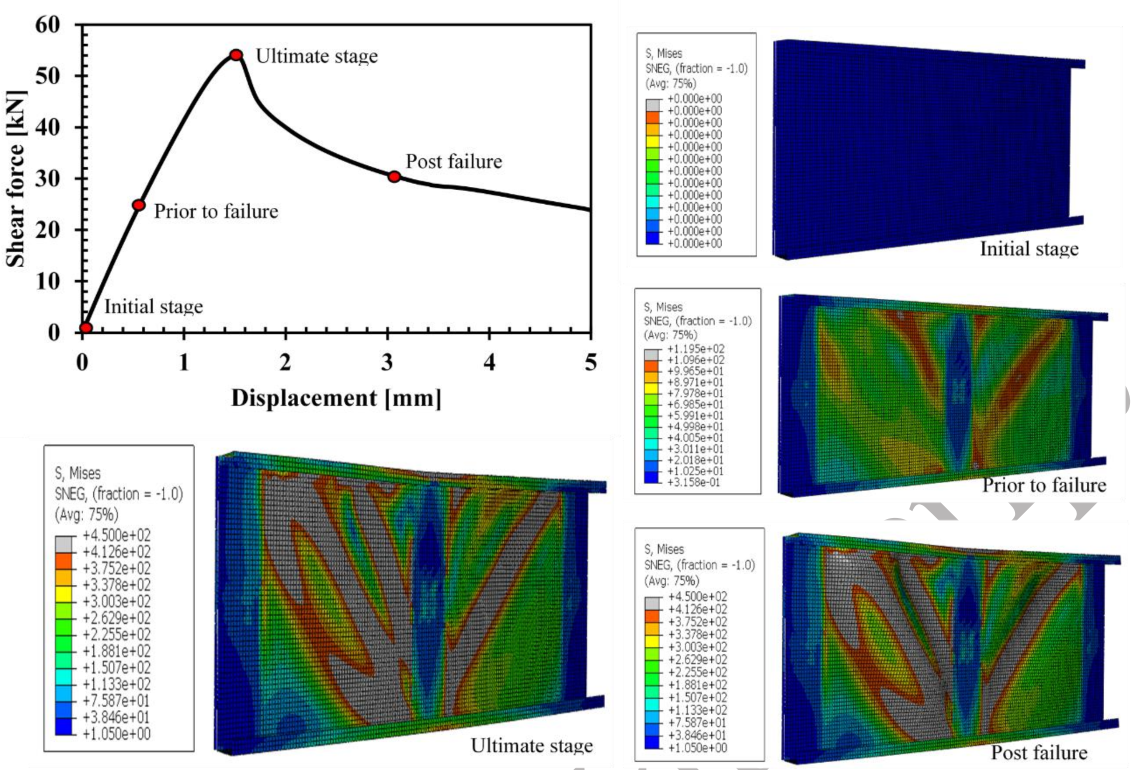

Fig. 14 Shear failure mode progression of optimised lipped channel beam for shear

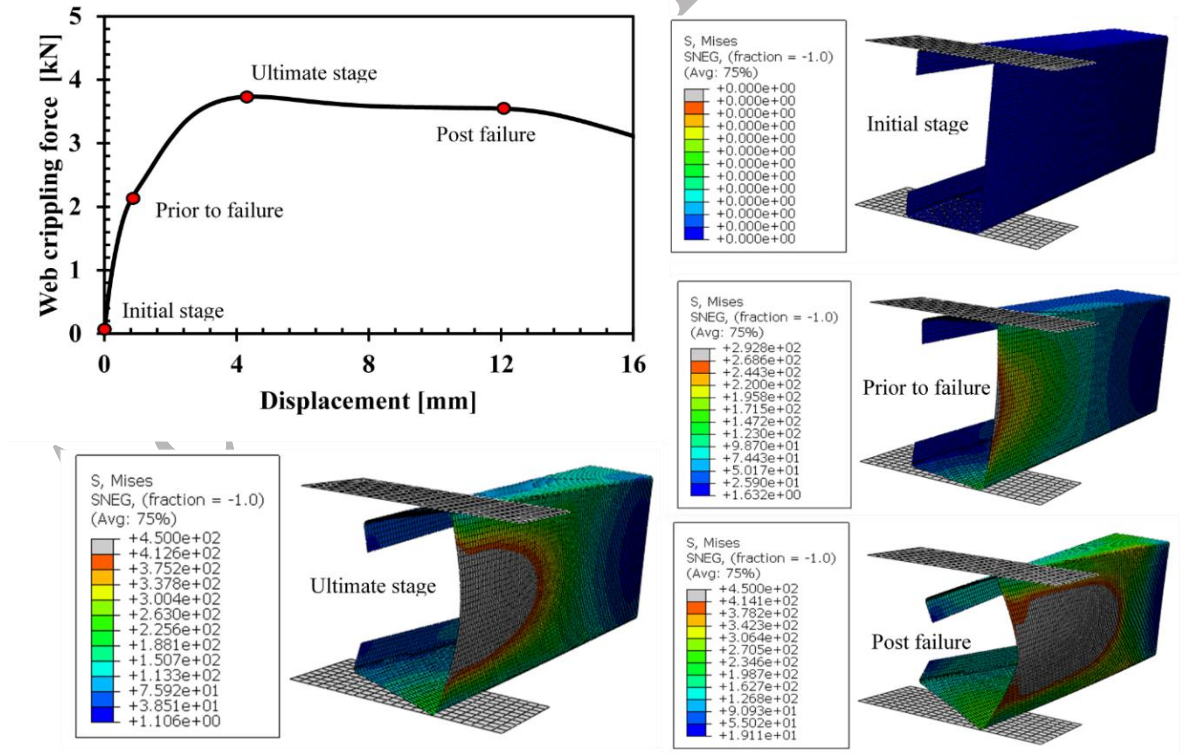

Fig. 15 Web crippling failure mode progression of optimised lipped channel beam for web crippling

Table 6: Comparison of the bending, shear, and web crippling capacities of optimised lipped channel beams obtained from Eurocode3 (EC3) and FE analysis.

Optimisation criteria	Optimised capacities and other capacities (Eurocode 3)			Optimised capacities and other capacities (FE analysis)			EC3 /FE		
	$M_{c,Rd}$ (kNm)	$V_{b,Rd}$ (kN)	$R_{w,Rd}$ (kN)	$M_{c,Rd}$ (kNm)	$V_{b,Rd}$ (kN)	$R_{w,Rd}$ (kN)	M_{EC3} / M_{FE}	V_{EC3} / V_{FE}	R_{EC3} / R_{FE}
Reference (Fig. 5)	10.30	47.92	4.16	10.41	53.70	3.09	0.99	0.89	1.35
Bending (Eq. 10)	13.38	49.96	3.75	13.28	54.32	2.76	1.01	0.92	1.36
Shear (Eq. 11)	12.51	50.63	3.59	11.76	54.97	2.56	1.06	0.92	1.40
Web crippling (Eq. 12)	8.62	44.33	4.68	7.95	48.80	3.74	1.08	0.91	1.25
Combined (Eq.13)	11.59	47.92	4.16	12.08	53.70	3.09	0.96	0.89	1.34
Mean							1.02	0.91	1.34
COV							0.055	0.014	0.047

Note: $M_{c,Rd}$ = Section moment capacity, $V_{b,Rd}$ = Shear resistance, $R_{w,Rd}$ = Web crippling strength.

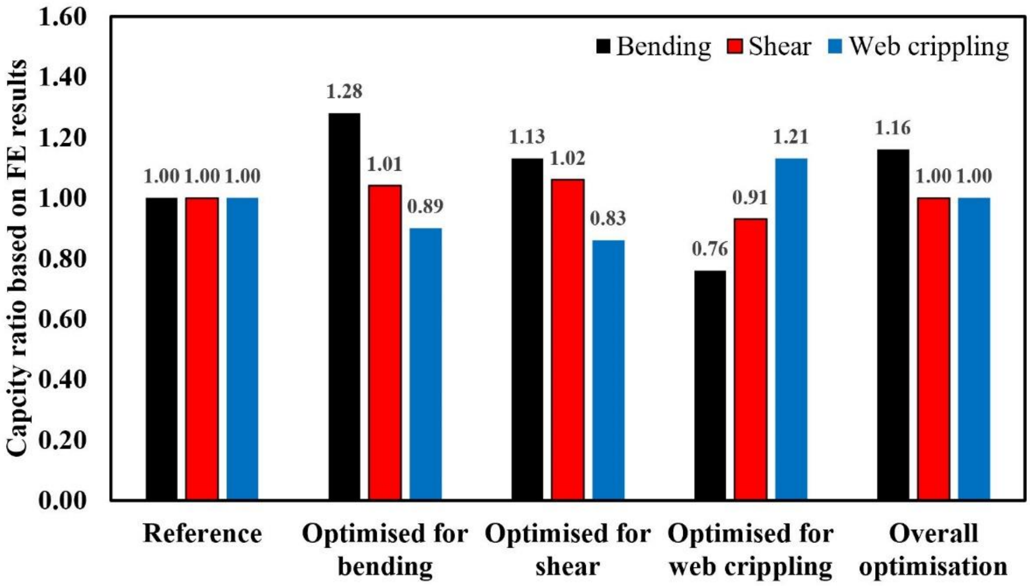

Fig. 16 Performance of the optimised lipped channel beams based on FE results

5 Discussion of results

Several observations were made while performing the optimisation process for bending, shear, web crippling, and combined actions. The optimisation for bending resulted in a relatively slender section of lipped channel beam and showed approximately a 30 % enhancement in the bending capacity over the same amount of material used. The optimised dimensions for bending also resulted in shear capacity enhancement of 4 % and web crippling strength reduction of 10% compared to reference lipped channel section. Optimising the dimensions intend to maximise the shear capacity registered only 6 % of the shear resisting capacity enhancement. In addition, the optimisation for shear reduces the web crippling capacity by 14% and enhancement in bending capacity by 21% compared to the reference lipped channel beam. Optimisation for web crippling resulted in 13 % of the web crippling capacity enhancement compared to the reference lipped channel beam. However, the performance of under bending and shear actions is relatively poor with 16% and 7 % reduction, respectively.

The overall optimisation strategy appeared to be acceptable, as it showed reasonable results without any reduction of the bending, shear, and web crippling capacities compared to reference lipped channel beam. The shear and web crippling capacities remained similar as the reference lipped channel beam, thus there was not any alteration in the dimension of the web compared to the reference section. This can be argued that shear capacity increases with web depth while web crippling capacity reduces with web depth. To satisfy both shear and web crippling, the optimisation resulted in similar dimensions for the web as a reference section. However, the flange and lipped dimensions varied themselves during the combined optimisation such that the lip reached the upper bound and the flange attained the remaining material thus maximising the second moment of area. However, the bending capacity enhancement was 12%, compared to reference lipped channel beam.

The accuracy of the optimisation results was examined by developing FE models. The developed FE models showed excellent agreement with the experiment results. The section moment capacities obtained from FE analyses showed satisfactory agreement with the capacities obtained using Eurocode 3 [18, 19] for the optimised sections. The EN1993-1-5 [19] shear predictions are, however, relatively conservative compared to FE results as EN1993-1-5 [19] does not consider the enhanced value of shear buckling coefficient due to the additional fixity in web-flange juncture as proposed in [5]. It is important to note that unsafe predictions for web crippling capacities were observed from EN1993-1-3 [18] compared to the FE results. Sundararajah et al. [4] have also acknowledged that EN1993-1-3 [18] prediction for web crippling strength under ETF and ITF load case are either over-conservative or unsafe. Therefore, shear and web crippling calculations appear in Eurocode 3 [18, 19] need an update.

It is finally proposed that based on the results obtained in this study the combined optimisation criteria suits well with ~12 % bending capacity increase without compromising the shear and web crippling capacities. Optimisation for bending criteria also suits well with enhancements in bending and shear capacities and only 10% reduction in web crippling capacity.

6 Conclusions

In this paper, the CFS lipped channel beam was optimised for combined bending, shear, web crippling using PSO algorithm. The ultimate capacity and structural behaviour of the optimised lipped channels also simulated using validated FE models. Based on the findings following conclusions can be drawn.

- The individual optimisation for bending, shear, and web crippling actions resulted in 30 %, 6 %, and 13 % of capacity increase, respectively compared to the reference section with the same amount of material.
- The newly proposed concept of combined optimisation resulted in the ~12 % bending capacity increase without compromising the shear and web crippling capacities.
- It is concluded that individual optimisation for bending and combined optimisation will both result in efficient lipped channel CFS beams.
- FE models predicted satisfactorily the section moment capacities of the optimised sections. Eurocode 3 calculations for shear and web crippling are conservative and unsafe, respectively compared to FE predictions.
- The combined performance of bending, shear, and web crippling can be enhanced using the proposed novel optimisation concept.

Acknowledgements

The authors would like to thank Northumbria University for financial support and providing necessary research facilities to conduct this research project.

References

[1] C.H. Pham, G.J. Hancock, Experimental Investigation and Direct Strength Design of High-Strength, Complex C-Sections in Pure Bending, Journal of Structural Engineering 139(11) (2013) 1842-1852.

[2] C. Yu, B.W. Schafer, Distortional buckling test on cold-formed steel beams, Journal of Structural Fire Engineering 132(4) (2006) 515-528.

[3] R. Siahaan, M. Mahendran, P. Keerthan, Section moment capacity tests of rivet fastened rectangular hollow flange channel beams, Journal of Constructional Steel Research 125 (2016) 252-262.

[4] L. Sundararajah, M. Mahendran, P. Keerthan, Experimental Studies of Lipped Channel Beams Subject to Web Crippling under Two-Flange Load Cases, Journal of Structural Engineering 142(9) (2016).

[5] P. Keerthan, M. Mahendran, Experimental investigation and design of lipped channel beams in shear, Thin-Walled Structures 86 (2015) 174-184.

[6] C.H. Pham, G.J. Hancock, Numerical simulation of high strength cold-formed purlins in combined bending and shear, Journal of Constructional Steel Research 66(10) (2010) 1205-1217.
[7] W.-X. Ren, S.-E. Fang, B. Young, Analysis and design of cold-formed steel channels subjected to combined bending and web crippling, Thin-Walled Structures 44(3) (2006) 314-320.
[8] L. Sundararajah, M. Mahendran, P. Keerthan, New design rules for lipped channel beams subject to web crippling under two-flange load cases, Thin-Walled Structures 119 (2017) 421-437.
[9] P. Keerthan, M. Mahendran, Numerical Modeling of LiteSteel Beams Subject to Shear, Journal of Structural Engineering 137(12) (2011) 1428-1439.
[10] M.R. Haidarali, D.A. Nethercot, Finite element modelling of cold-formed steel beams under local buckling or combined local/distortional buckling, Thin-Walled Structures 49(12) (2011) 1554-1562.
[11] K. Roy, H.H. Lau, T.C.H. Ting, B. Chen, J.B.P. Lim, Flexural capacity of gapped built-up cold-formed steel channel sections including web stiffeners, Journal of Constructional Steel Research 172 (2020).
[12] A. Uzzaman, J.B.P. Lim, D. Nash, K. Roy, Cold-formed steel channel sections under end-two-flange loading condition: Design for edge-stiffened holes, unstiffened holes and plain webs, Thin-Walled Structures 147 (2020).
[13] J. Ye, I. Hajirasouliha, J. Becque, K. Pilakoutas, Development of more efficient cold-formed steel channel sections in bending, Thin-Walled Structures 101 (2016) 1-13.
[14] J. Ye, I. Hajirasouliha, J. Becque, A. Eslami, Optimum design of cold-formed steel beams using Particle Swarm Optimisation method, Journal of Constructional Steel Research 122 (2016) 80-93.
[15] G. Perampalam, K. Poologanathan, S. Gunalan, J. Ye, B. Nagaratnam, Optimum Design of Cold-formed Steel Beams: Particle Swarm Optimisation and Numerical Analysis, ce/papers 3(3-4) (2019) 205-210.
[16] P. Gatheeshgar, K. Poologanathan, S. Gunalan, B. Nagaratnam, K.D. Tsavdaridis, J. Ye, Structural behaviour of optimized cold-formed steel beams, Steel Construction (2020).
[17] P. Gatheeshgar, P. Keerthan, G. Shanmuganathan, T. Konstantinos Daniel, N. Brabha, I. Eleni, Optimised cold-formed steel beams in modular building applications, Journal of Building Engineering (In press) (2020).
[18] CEN, Eurocode 3 - Design of steel structures - Part 1-3 General rules- Supplementary rules for cold-formed members and sheeting, European Comittee for Standardization, Brussels, 2006.
[19] CEN, Eurocode 3 - Design of steel structures - Part 1-5, Plated structural elements, European Commitee for Standardization Brussels, 2006.
[20] D.M.M.P. Dissanayake, K. Poologanathan, S. Gunalan, K.D. Tsavdaridis, B. Nagaratnam, K.S. Wanniarachchi, Numerical modelling and shear design rules of stainless steel lipped channel sections, Journal of Constructional Steel Research (2019).
[21] J. Lee, S.-M. Kim, H.-S. Park, B.-H. Woo, Optimum design of cold-formed steel channel beams using micro Genetic Algorithm, Engineering Structures 27(1) (2005) 17-24.
[22] ABAQUS, Hibbitt, Karlsson & Sorensen, Inc., Paw-tucket, USA, 2017.
[23] B.W. Schafer, T. Pekoz, Computational modeling of cold-formed steel: characterizing geometric imperfections and residual stresses, Journal of Constructional Steel Research 47 (1998) 193-210.
[24] R. Siahaan, P. Keerthan, M. Mahendran, Finite element modeling of rivet fastened rectangular hollow flange channel beams subject to local buckling, Engineering Structures 126 (2016) 311-327.
[25] P. Keerthan, M. Mahendran, New design rules for the shear strength of LiteSteel beams, Journal of Constructional Steel Research 67(6) (2011) 1050-1063.
[26] B.W. Schafer, Z. Li, C.D. Moen, Computational modeling of cold-formed steel, Thin-Walled Structures 48(10-11) (2010) 752-762.
[27] N. Degtyareva, P. Gatheeshgar, K. Poologanathan, S. Gunalan, M. Lawson, P. Sunday, Combined bending and shear behaviour of slotted perforated steel channels: Numerical studies, Journal of Constructional Steel Research 161 (2019) 369-384.
[28] P. Keerthan, M. Mahendran, D. Hughes, Numerical studies and design of hollow flange channel beams subject to combined bending and shear actions, Engineering Structures 75 (2014) 197-212.